

Evolutionary constraints mediate extinction risk under climate change

Guillermo Garcia Costoya¹, Claire Williams¹, Trevor Faske¹, Jacob Moorman², and Michael Logan¹

¹University of Nevada Reno

²University of California Los Angeles

October 11, 2022

Abstract

Mounting evidence suggests that rapid evolutionary adaptation may rescue some organisms from the impacts of ongoing climate change. However, evolutionary constraints might hinder this process, especially when different aspects of environmental change generate antagonistic selection on genetically correlated traits. Here, we use individual-based simulations to explore how genetic correlations underlying the thermal physiology of ectotherms might influence their responses to the two major concomitant components of climate change—increases in mean temperature and thermal variability. We found that genetic correlations can influence population dynamics under climate change, with declines in population size varying three-fold depending on the type of correlation present. Surprisingly, populations whose thermal performance curves were constrained by genetic correlations often declined less rapidly than unconstrained populations. Our results suggest that accurate forecasts of the impact of climate change on ectotherms will require an understanding of the genetic architecture of the traits under selection.

1 **Title Page:**

2

3 **Article Title:** Evolutionary constraints mediate extinction risk under climate change

4 **Authors:** Guillermo Garcia-Costoya¹, Claire E. Williams¹, Trevor M. Faske¹, Jacob D.
5 Moorman², Michael L. Logan¹.

6 **Author e-mails (same order):** guille@nevada.unr.edu, williams.claire.e@gmail.com,
7 tfaske@nevada.unr.edu, jacob@moorman.me, michaellogan@unr.edu

8 **Affiliations:** ¹University of Nevada, Reno, Reno, NV, USA, ²University of California, Los
9 Angeles, CA, USA

10 **Running title:** Evolutionary constraints and climate change

11 **Keywords:** genetic correlation, thermal physiology, climate change, evolutionary constraint,
12 extinction risk.

13 **Type of article:** Letter

14 **Abstract word count:** 144

15 **Main text word count:** 4396

16 **Number of figures:** 3

17 **Number of references:** 65

18 **Corresponding author:** Guillermo Garcia-Costoya, guille@nevada.unr.edu, +1 (775) 247-
19 4284

20 **Statement of authorship:** GGC and MLL conceptualized the project. GGC, TMF, CEW and
21 JDM developed the simulation code, GGC wrote the first draft of the manuscript and all authors
22 contributed to manuscript revision.

23 **Data accessibility statement:** All scripts used for this manuscript are available on GitHub at:
24 https://github.com/ggcostoya/tpc_genetic_correlations.

25 The original data for populations, climate change scenarios and simulation outcomes are stored
26 temporarily on Google Drive at:

27 <https://drive.google.com/drive/folders/1nxoNiDcqxyInwjXeWqUe5b4KYCWmzzBf?usp=sharing>
28 [g](#). Metadata and links to these files are also available through the GitHub repository and upon
29 publication of the manuscript they will be made available and archived in an appropriate public
30 repository.

31

32

33 **Abstract:**

34 Mounting evidence suggests that rapid evolutionary adaptation may rescue some organisms from
35 the impacts of climate change. However, evolutionary constraints might hinder this process,
36 especially when different aspects of environmental change generate antagonistic selection on
37 genetically correlated traits. Here, we use individual-based simulations to explore how genetic
38 correlations underlying the thermal physiology of ectotherms might influence their responses to
39 the two major components of climate change—increases in mean temperature and thermal
40 variability. We found that genetic correlations can influence population dynamics under climate
41 change, with declines in population size varying three-fold depending on the type of correlation
42 present. Surprisingly, populations whose thermal performance curves were constrained by
43 genetic correlations often declined less rapidly than unconstrained populations. Our results
44 suggest that accurate forecasts of the impact of climate change on ectotherms will require an
45 understanding of the genetic architecture of the traits under selection.

46

47

48

49

50

51

52

53

54

55

56 **Main Body:**

57 **Introduction**

58 Global climate change is a major threat to life on Earth, with climate models predicting
59 continued increases in both the mean and variability of environmental temperature (Allan et al.,
60 2021; Bathiany et al., 2018). Ongoing shifts in thermal environments have already been linked to
61 negative impacts on organisms and have resulted in dramatic declines in many taxonomic groups
62 (Bellard et al., 2012; Sinervo et al., 2010). As climate change progresses, organisms must
63 respond to these pressures in order to persist. Organismal responses can occur in various ways,
64 including range shifts (Booth et al., 2011; Elmhagen et al., 2015), behavioral or phenological
65 modifications (Fey et al., 2019; Kearney et al., 2009), or acclimatization (Charmantier et al.,
66 2008; Cohen et al., 2018; Ovaskainen et al., 2013). Nonetheless, species for which these
67 mechanisms are insufficient (e.g., species with limited dispersal capacity) must rely on *in situ*
68 genetic adaptation to survive (Hairston et al., 2005; Hoffmann & Sgrò, 2011).

69 A range of intrinsic and extrinsic variables determine the ability of populations to evolve
70 rapidly in the face of shifting thermal environments. First, the opportunity for natural selection
71 is limited by the amount of phenotypic diversity within a population, while the efficacy of
72 selection (i.e., the evolutionary response) is mediated by the heritability and genetic architecture
73 of the relevant traits (Fisher, 1958). Large populations typically have greater levels of both
74 phenotypic and genetic variation, and they have more individuals by which to resist selection
75 load — the increased mortality and drop in population size that can arise from strong selection
76 (Frankham, 1996; Lande, 1993). Nonetheless, even in large populations, traits may be
77 genetically correlated in ways that either enhance or constrain the response to selection (Chevin,
78 2013; Kingsolver & Diamond, 2015; Logan & Cox, 2020; Schou et al., 2022). Thus, genetic

79 correlations may impact population dynamics as environments change, but this possibility has
80 largely been overlooked in the climate-impact literature.

81 Genetic correlations are the result of relationships between traits at the genetic level and
82 can arise through ultimate (evolutionary) mechanisms like correlational selection (Roff &
83 Fairbairn, 2012) and proximate (developmental) mechanisms like pleiotropy or linkage
84 disequilibrium (Hochachka & Somero, 2002). Genetic correlations result in limitations to the
85 space and direction along which phenotypes vary in a population (Chevin, 2013). Consequently,
86 identifying how genetic correlations mediate rapid evolutionary change in climate-related traits
87 is crucial for accurately predicting organismal responses to climate change. Indeed, because
88 climate change represents at least two distinct axis of environmental change (increasing mean
89 and variance of environmental temperature) that serve as agents of selection on different traits,
90 genetic correlations among these traits may play a disproportionate role in the dynamics of
91 adaptation (Logan & Cox, 2020).

92 Climate forecasts project that mean environmental temperature will increase globally
93 between 1 and 3°C by the end of the 21st century (Allan et al., 2021). A similar pattern has been
94 predicted for thermal variability, with an expected 15% increase in standard deviation for every
95 1°C increase in mean temperature (Bathiany et al., 2018). These changes may be especially
96 profound for ectotherms due to their inability to regulate internal body temperature using
97 physiological means. The primary traits that dictate an ectotherm's relationship with its thermal
98 environment are those that underly the thermal performance curve (TPC). For ectotherms, TPCs
99 are functions that describe the relationship between body temperature to performance or fitness
100 (Angilletta, 2009; Huey & Stevenson, 1979), and the parameters of these curves can be
101 considered traits that combine to describe their shape. The thermal optimum (T_{opt}) is the body

102 temperature where maximum performance (P_{\max}) is achieved. The critical thermal minimum
103 (CT_{\min}) and maximum (CT_{\max}) are known as the critical thermal limits and are the body
104 temperatures where performance drops to zero. The critical thermal limits, along with the
105 magnitude of increase and decrease in performance with increasing temperature below and above
106 T_{opt} , respectively, jointly determine the breadth of the TPC (T_{br} ; Figure 1A). An increase in mean
107 environmental temperature should select for an increase in T_{opt} (Logan et al., 2014), whereas an
108 increase in thermal variability should select for lower CT_{\min} , higher CT_{\max} , and a wider T_{br}
109 (Gilchrist, 1995). Thus, in the absence of constraints, climate change should result in the
110 evolution of broader TPCs with higher thermal optima.

111 Nevertheless, two major categories of genetic correlations that constrain TPC shapes
112 have been identified in natural populations of ectotherms. These are the “generalist-specialist
113 trade-off” (GSTO) and the “thermodynamic effect” (TDE; also known as the “hotter-is-better”
114 hypothesis). A GSTO is present when the area under the TPC remains constant despite shifts in
115 TPC shape (Figure 1B), and this pattern has been observed in many species at the phenotypic
116 level (Condon et al., 2015; Gilchrist, 1996; Gilchrist et al., 1997; Kingsolver et al., 2015; Latimer
117 et al., 2011; Phillips et al., 2014; Richter-Boix et al., 2015). Aspects of the GSTO, including
118 negative correlations between CT_{\min} and CT_{\max} or between P_{\max} and T_{br} have also been
119 documented at the genetic level in some species (Berger et al., 2014; Izem & Kingsolver, 2005;
120 Kingsolver et al., 2004; Knies et al., 2006). The GSTO is thought to occur because of the
121 antagonistic pleiotropy that arises from the cost imposed by maximizing performance in the local
122 thermal environment (i.e., “a jack of all environments is a master of none”; Gilchrist, 1996). A
123 TDE is present when there is a positive correlation between T_{opt} and P_{\max} (Figure 1C). As with
124 the GSTO, the TDE has been observed at both the phenotypic (Knies et al., 2009; Phillips et al.,

125 2014) and genetic (Bennett et al., 1992; Berger et al., 2014) levels and is thought to arise because
126 biochemical reaction rates are more efficient at warmer temperatures (Angilletta et al., 2010).
127 Furthermore, growing evidence suggests that both the GSTO and TDE can occur within the same
128 population (Gilchrist, 1996; Logan et al., 2018; Logan & Cox, 2020; Martins et al., 2019; Figure
129 1D) raising the possibility that some populations might be able to adapt to either rising mean
130 temperatures or increasing thermal variability, but not both (Logan et al., 2020; Logan & Cox,
131 2020). These types of genetic correlations may be ubiquitous in natural populations and could
132 have important effects on the evolutionary potential of ectotherms under climate change.

133 Here, we examined the role of genetic correlations in the responses of ectotherms to
134 multidimensional climate change using individual-based simulations. First, we generated a set of
135 populations of ectotherms differing in the genetic correlations constraining their TPC shapes and
136 in initial population size. Then, we exposed them to climate change scenarios of varying
137 magnitudes following IPCC predictions, tracking trait evolution and changes in population size
138 over 80 generations. We hypothesized that genetic correlations would affect extinction
139 probabilities in a rank-order fashion in the following way: 1) populations whose TPCs were
140 constrained only by the TDE would fare the best, followed by 2) populations with no genetic
141 correlations at all, 3) populations that were constrained only by the GSTO, and finally, 4)
142 populations constrained by both the TDE and the GSTO. We also hypothesized that extinction
143 would occur fastest in populations with the smallest initial size, but that the relative vulnerability
144 of populations exposed to a given set of genetic constraints would be consistent irrespective of
145 starting population size. Our analysis represents, to our knowledge, the first attempt to simulate
146 the role of genetic constraints on rapid adaptation and extinction risk under contemporary

147 climate change and has important implications for understanding the vulnerability of ectotherms
148 to rapid environmental change.

149

150 **Methods**

151 To examine the role of genetic correlations in the responses of ectotherms to climate change, we
152 conducted individual-based simulations that challenged populations of a hypothetical
153 ectothermic animal with increasingly warmer and variable thermal environments. Each
154 individual was defined exclusively by their thermal performance curve (TPC), making the match
155 between the shape of their TPC and the environmental temperature the sole determinant of their
156 performance and ultimately their survival and reproduction. For some simulations, we introduced
157 genetic correlations that limited the possible range of shapes that TPCs within a population could
158 assume.

159 We considered a hypothetical ectotherm species that, like many insects and small
160 vertebrates, had an annual reproductive cycle with non-overlapping generations. Our organism
161 reproduced asexually via perfect cloning (i.e., the narrow-sense heritability of TPC parameters
162 was 1). We did not allow mutation to occur, as theoretical and empirical work has demonstrated
163 that the majority of adaptive evolution over short timescales occurs via changes in standing
164 genetic variation (Barrett & Schluter, 2008; Burke et al., 2014; Chaturvedi et al., 2021;
165 Schlötterer et al., 2015; Teotónio et al., 2009). Our hypothetical ectotherm was a
166 thermoconformer, meaning that the environmental temperatures they experienced were
167 equivalent to their body temperatures. Lastly, populations evolved in a closed environment (i.e.,
168 no gene flow) that was thermally homogeneous in space. We generated 120 unique starting
169 populations whose TPCs were subject to one of four genetic correlation scenarios: 1) no genetic

170 correlations, 2) generalist-specialist trade-off (GSTO), 3) thermodynamic effect (TDE), and 3)
171 both a specialist-generalist trade-off and a thermodynamic effect (GSTO + TDE; Figure 1).
172 Within each genetic correlation scenario, we ran simulations with three different initial
173 population sizes ($N_0 = 50$, $N_0 = 500$ & $N_0 = 5000$), and we set carrying capacity (K) equal to N_0 .
174 After allowing acclimatization to an initially stable environment for five generations, populations
175 were exposed to changing thermal regimes for 80 generations (through the end of the century),
176 following the global average predictions of the three main IPCC climate change scenarios: RCP
177 4.5, RCP 6, and RCP 8.5 (IPCC 2021, Allan et al., 2021). In this primary set of simulations, both
178 the mean and variability of temperature increased simultaneously following climate forecasts.
179 We further isolated the role of changing mean temperature versus changing thermal variability
180 by conducting an additional set of simulations where we allowed only the mean or the variability
181 to change. As each simulation unfolded, we recorded changes in population size, extinction rate,
182 and the evolution of TPCs.

183 Further details on the processes of generating the starting populations, simulating thermal
184 environments, and the modelling of survival and reproduction, can be found in the
185 supplementary materials. All code for this manuscript was written using the R language (R Core
186 Team 2021). Simulations were run on a high-performance computing cluster at the University of
187 Nevada, Reno.

188

189 **Results**

190 Our hypothetical ectotherm populations were able to withstand the two least severe climate
191 change scenarios, irrespective of the genetic correlations present (RCP 4.5 and RCP 6). On
192 average, with respect to the initial size and across all simulations challenged with a particular

193 climate change scenario, population sizes decreased by only 3% and 6% for the RCP 4.5 and
194 RCP 6 scenario. These declines were similar to the control scenario where no environmental
195 change occurred and average population size did not decrease at all (Figure 2, Figure S1A, Table
196 S1). Nonetheless, for the more severe RCP 8.5 scenario, population size decreased on average by
197 56%, indicating a much higher likelihood of extinction if climate change progresses via this
198 worst-case scenario (Figure 2, Table S1).

199 Changes in mean and/or standard deviation also produced different patterns of population
200 decline. For the RCP 8.5 scenario, when we allowed only mean temperature (Figure S1D) or
201 thermal variability (Figure S1E) to change, increases in mean temperature (average decline of
202 19%) were more detrimental than increases in standard deviation (no decline). When further
203 exploring the influence of thermal variability, we saw that a more variable initial thermal
204 environment (initial $T_{sd} = 2^{\circ}\text{C}$ instead of 1°C), but with no changes in thermal conditions over
205 time, led to frequent fluctuations in population size by the end of the simulation, indicating that
206 populations were maladapted to starting conditions but were able to persist by adapting over time
207 (Figure S1B). If we allowed thermal conditions to change following the RCP 8.5 scenario, an
208 initially more thermally variable environment always resulted in extinction by the 80th generation
209 of change (Figure S1C).

210 Unsurprisingly, initial population size played an important role in mediating extinction
211 risk. Populations of $N_0 = 50$ declined by an average of 37% after 80 generations of change
212 (across all scenarios excluding the control; Figure 2A-C, Table S1). In contrast, populations of
213 $N_0 = 500$ and $N_0 = 5000$ declined by an average of 15% and 13%, respectively (Figure 2D-I,
214 Table S1).

215 Genetic correlations played an important role in determining the extent of population
216 decline. Populations subject to the GSTO experienced the most severe population size declines
217 (average decline of 35%) closely followed by populations subject to no genetic correlations at all
218 (average decline of 33%). Populations subject to the TDE performed best, only declining by an
219 average of 11%. Populations subject to both the GSTO and the TDE declined by an average of
220 17% (Figure 2, Table S1). Despite notable differences in population decline depending on the
221 type of genetic constraint present, all populations followed similar trajectories with respect to
222 changes in average reproductive success, regardless of the particular combination of climate
223 change scenario and genetic constraint. Mean reproductive success increased in early stages
224 (generations 0-20) but then declined continuously until the end of the simulation with varying
225 degrees of intensity depending on the genetic constraints present and the climate change scenario
226 (Figure 3A, S3A, S4A).

227 As expected, TPC shape evolved in response to environmental change. By the end of our
228 simulations, CT_{\min} , T_{opt} , CT_{\max} and P_{\max} had increased by an average of 0.6 °C, 1.8 °C, 0.25 °C,
229 and 2.23, and by 0.6 °C, 2.1 °C, 0.7 °C, and 2.15 for the worst climate change scenario we
230 considered (RCP 8.5, Table S3). Initially, TPCs with high values of both P_{\max} and T_{opt} were
231 favored by selection across all simulations. However, the particular set of genetic correlations
232 present in a given set of simulations affected the ability of populations to achieve local fitness
233 optima. For example, in the initial generations, GSTO + TDE constrained populations achieved
234 the highest values of P_{\max} , whereas populations subjected to only the TDE achieved the highest
235 values of T_{opt} . Populations whose TPCs were unconstrained by genetic correlations achieved
236 comparatively low values of both of these traits in the early stages of the simulation.
237 Additionally, the relationships between traits imposed by genetic correlations resulted in the

238 correlated evolution of these traits. For GSTO and GSTO + TDE constrained populations, CT_{\min}
239 and CT_{\max} increased and decreased, respectively, due to the loss in thermal breadth associated
240 with gains in P_{\max} . In contrast, the TPCs of populations that were unconstrained by genetic
241 correlations evolved to be broader. In other words, unconstrained populations evolved towards
242 generalism (lower CT_{\min} and higher CT_{\max}) as the simulation unfolded (Figure 3B-D, S3B-D,
243 S4B-D, Table S3).

244

245 **Discussion**

246 As climate change progresses, organisms will be faced with novel selection pressures that might
247 require *in situ* adaptation (Hairston et al., 2005; Hoffmann & Sgrò, 2011). However, the potential
248 for evolutionary rescue depends on several factors, including the presence and structure of
249 genotypic and phenotypic variation (Chevin, 2013; Kingsolver & Diamond, 2015). Genetic
250 correlations, which are known to occur between traits that underly the thermal performance
251 curves of ectotherms, might influence evolutionary (and therefore, population) responses, but the
252 ways in which this might occur have not been previously tested. Our simulations revealed that
253 evolutionary constraints in the form of genetic correlations might influence the ability of
254 ectotherms to adapt to climate change, especially when the rate of change in thermal
255 environments is high. Surprisingly, and in disagreement with our *a priori* hypotheses, genetic
256 correlations often increased adaptive potential. Finally, we found that the specific ways in which
257 thermal environments shifted (i.e., changing mean temperature versus thermal variability) had
258 strong effects on extinction probabilities.

259 There is ample empirical evidence that TPCs of wild organisms are subject to phenotypic
260 correlations that follow the GSTO and TDE. While the mechanisms that underly these

261 phenotype-level patterns are less clear, growing evidence suggests that genetic correlations are at
262 play in at least some cases (Angilletta et al., 2010; Berger et al., 2014; Condon et al., 2015;
263 Gilchrist, 1996; Gilchrist et al., 1997; Izem & Kingsolver, 2005; Kingsolver et al., 2004, 2015;
264 Knies et al., 2006, 2009; Latimer et al., 2011). A few studies have even presented evidence of
265 both the GSTO and TDE occurring at the genetic level in the same population (Logan et al.,
266 2020; Martins et al., 2019). In our study, we hypothesized that the limitations on phenotypic
267 variability caused by genetic correlations like the TDE could be beneficial in adapting to climate
268 change while others like the GSTO might be detrimental. We also hypothesized that the
269 combination of these two types of genetic correlation would be the most harmful, leading to the
270 rapid evolution of specialization (increasing T_{opt} leading to increasing P_{max} which in turn leads to
271 decreasing T_{br}) followed by population extinction in later stages when thermal environments
272 become highly variable. Finally, we hypothesized that unconstrained TPC evolution (the
273 complete absence of genetic correlations) would decrease the likelihood of extinction compared
274 to every genetic correlation scenario except for the TDE.

275 With respect to populations constrained by either the TDE or the GSTO, our simulations
276 predicted outcomes similar to what we had hypothesized. Populations subjected to the TDE
277 declined the least across all climate change scenarios whereas the GSTO-constrained populations
278 declined the most (Figure 2). Among populations subjected to the TDE and no other genetic
279 correlation, the initial environment favored individuals with high P_{max} that, due to the genetic
280 correlation, also had higher T_{opt} (Figure 3, Figure S2H). In early stages of environmental change,
281 this correlation between traits decreased the degree of overlap between the populations' average
282 TPC and the distribution of environmental temperatures leading to lower reproductive success.
283 Nonetheless, the initial increase in T_{opt} produced TDE populations that were pre-adapted to the

284 much warmer environment that would emerge in later generations (Figure 3C). Our results agree
285 with previous studies which suggest that the gains in performance offered by the TDE (e.g.,
286 through increased reproductive or developmental rates; Walters et al. 2012), might offer some
287 ectotherms an advantage in the face of climatic change (Angilletta et al. 2010, Walters et al.
288 2012, Logan & Cox 2020).

289 Among populations subject to the GSTO and no other genetic correlation, natural
290 selection also favored high P_{\max} phenotypes before substantial environmental change had
291 occurred, however, this had a two-fold negative impact. First, due to the GSTO, individuals with
292 high P_{\max} values that were favored in early generations had reduced TPC breadth which left them
293 vulnerable to increasing thermal variability. Second, individuals with T_{opt} values matching the
294 mean temperature of the starting thermal environment were heavily favored, leading to an early
295 loss of heat-adapted individuals. These two circumstances ultimately led to the rapid evolution of
296 “cold-adapted” specialists (i.e., adapted to the historically cooler thermal environment) and made
297 GSTO-constrained populations susceptible to increases in both mean temperature and thermal
298 variability (Figure 3). The GSTO is by far the most common genetic constraint found in
299 ectotherm populations (Logan et al. 2020), and thus may represent an important driver of
300 extinction risk in nature.

301 Populations subject to both the GSTO and TDE, as well as those subjected to no genetic
302 correlations at all, did not follow our *a priori* hypotheses. For example, when populations were
303 constrained by both types of correlations, they did better than when they were only constrained
304 by the GSTO, suggesting that the adaptive benefits conferred by the TDE might outweigh the
305 limitations imposed by the GSTO (Figure 2). As previously mentioned, the GSTO promoted an
306 increase in P_{\max} and a decrease in TPC breadth during the early stages of adaptation. Nonetheless,

307 the presence of the TDE palliated the effects of maladaptation to warmer environments by
308 forcing high P_{\max} individuals to also have higher T_{opt} . In other words, when both genetic
309 correlations are present, heat-adapted individuals are retained in early generations (Figure 3).

310 Surprisingly, populations that were unconstrained by genetic correlations fared worse
311 than almost any set of populations where genetic correlations were present (unconstrained
312 populations performed similarly to those subject to the GSTO; Figure 2). The comparatively high
313 extinction likelihood of genetically unconstrained populations was due to the absence of
314 mechanisms allowing the existence of phenotypes with enhanced performance and reproductive
315 success in the earlier stages of the simulation (Figure 3, Figure S2A-C). Compared to
316 unconstrained populations, GSTO-constrained populations experienced enhanced reproductive
317 output at the beginning of simulations because the specialist individuals that were favored by
318 selection also had higher maximal performance (Figure 3). This increase in early reproductive
319 capacity among GSTO-constrained populations ultimately led to similar extinction probabilities
320 of GSTO-constrained and unconstrained populations even though the former populations
321 declined faster during the later stages of the simulations (Figure 2). This result highlights the role
322 of early local adaptation influencing longer term extinction probabilities via effects on
323 population size and highlights the fact that genetic correlations can be benign or even beneficial.
324 It is important to note, however, that GSTO-constrained populations did worse than
325 unconstrained populations when we doubled thermal variability at the start of simulations
326 (Figure S1C), indicating that selection for broader TPCs in these highly variable thermal
327 environments resulted in heavily reduced maximal performance capacity that prevented
328 evolutionary rescue.

329 What are the respective roles of changing mean temperature versus increasing thermal
330 variability in driving extinction risk? We explored this question by running a set of simulations
331 where either mean temperature or thermal variability was allowed to increase while the other
332 variable remained constant. Changes in thermal variability alone did not have negative impacts
333 on any of our populations (Figure S1D). On the other hand, changes in mean temperature did
334 have a negative impact, but only on those populations subjected to the GSTO or to no genetic
335 correlations at all (Figure S1E). Our results suggest that ectotherms with some genetic
336 architectures may be more limited by an ability to adapt to warmer environments than to more
337 variable ones. While previous studies have suggested that increasing thermal variability will play
338 an important role in driving population decline (Clusella-Trullas et al., 2011; Deutsch et al.,
339 2008; Vasseur et al., 2014), our simulations suggest that it is the synergistic effects of both
340 increasing mean temperature and thermal variability, rather than either on their own, that will
341 most profoundly influence extinction risk. With that said, we also note that thermal variability
342 played a much stronger role when the initial environment started out more thermally variable. It
343 was these simulations in which all populations went extinct, regardless of whether they were
344 constrained by genetic correlations (Figure S1C).

345 As we hypothesized, our simulations showed that larger population sizes and carrying
346 capacities reduced extinction probabilities (Figure 2). For any given set of genetic correlations,
347 starting population size interacted with the rate of climate change to determine the relative
348 vulnerability of populations. For starting populations sizes of 50, a large percentage of
349 populations went extinct by 2100, whereas many fewer went extinct when the starting population
350 size was 500 or 5000. Population size plays a dominant role in maintaining genetic and
351 phenotypic variation and is often considered the most important predictor of extinction risk in

352 changing environments (O’Grady et al., 2004). The greater phenotypic variation afforded by
353 higher population size increases the opportunity for selection and decreases the risk posed by
354 stochastic events (Fisher, 1958; Frankham, 1996; Lande, 1993).

355 Our analyses have several caveats that must be considered when attempting to extrapolate
356 our results to real world systems. First, our hypothetical ectotherm populations were modeled as
357 populations of TPCs. In real populations, TPC traits might correlate or trade-off with other traits
358 that themselves may be under selection as climate change progresses. In other words, there are
359 potentially many other relevant genetic correlations interacting with complex selection surfaces
360 that we did not consider in this study. For example, individuals with higher values of T_{opt} might
361 also be bolder, and if bolder individuals are more susceptible to predation, negative selection on
362 boldness might counteract the positive selection on T_{opt} , leading to zero evolutionary change in
363 either trait and generating different extinction probabilities from the ones presented here. Future
364 empirical and theoretical studies would benefit from considering these sorts of “complex
365 phenotypes” and how they may affect population dynamics in changing environments. Second,
366 our populations evolved in a spatially homogeneous thermal environment. While many
367 ectotherms live in these kinds of environments (e.g., tropical forest species; Logan et al., 2021;
368 Neel et al., 2021) and therefore thermoconform, many others live in spatially heterogenous
369 thermal environments that permit behavioral thermoregulation (Sears et al., 2016; Sears &
370 Angilletta, 2015). Behavioral thermoregulation is likely to reduce the strength of selection on
371 TPCs (a phenomenon termed the ‘Bogert Effect’; Huey et al., 2003, Logan et al., 2019, Muñoz,
372 2022) while reducing population decline, at least during earlier periods of environmental change
373 (Buckley et al., 2015). Simulations that examine population dynamics and the evolution of TPCs
374 in spatially heterogenous environments where individuals are allowed to thermoregulate are

375 likely to be informative. Third, our populations reproduced clonally with perfect heritability (i.e.,
376 genotypes and phenotypes were identical). Yet variation in most traits is driven, at least in part,
377 by local environmental effects. As with behavioral thermoregulation, plasticity in TPCs might
378 shield organisms from selection as climate change progresses but it could ultimately facilitate
379 adaptation via genetic accommodation (Chevin et al., 2013). The role of plasticity in genetic
380 evolution and population dynamics in changing environments is a rapidly growing area of
381 research (Fox et al., 2019), and future simulations could explore these dynamics by defining a set
382 of reaction norms that are applied to populations of TPCs experiencing changing thermal
383 environments. Despite these important caveats, our simulations provide a deep first attempt and
384 understanding the role of genetic correlations in the vulnerability of ectotherms to climate
385 change.

386 Through individual-based simulations, we showed that extinction risk under rapid climate
387 change may be mediated by several types of genetic correlations that are frequently observed to
388 underly the thermal performance curves of real populations. Further, these genetic correlations
389 usually enhanced survival relative to populations that are unconstrained by genetic correlations,
390 and the magnitude of these beneficial effects depend on the specific nature of environmental
391 change. Although recent studies have emphasized the importance of changing thermal variability
392 in generating extinction risk, our simulations suggest that increases in thermal variability on their
393 own may have little impact, but instead act synergistically with increasing mean temperatures to
394 threaten organisms. In summary, our results highlight the importance of treating climate change
395 as multi-dimensional and considering the genetic architecture of the traits under selection when
396 predicting extinction risk.

397

398 **Acknowledgements**

399 We thank Lutz Fromhage, Eric Riddell, Christian Cox, Jennifer Heppner, José F. García-
400 Martínez and the EvolDoers discussion group at the University of Nevada Reno for helpful
401 comments on the manuscript.

402

403 **References**

- 404 Allan, R. P., Hawkins, E., Bellouin, N., & Collins, B. (2021). *IPCC, 2021: Summary for*
405 *Policymakers* (V. Masson-Delmotte, P. Zhai, A. Pirani, S. L. Connors, C. Péan, S.
406 Berger, N. Caud, Y. Chen, L. Goldfarb, M. I. Gomis, M. Huang, K. Leitzell, E. Lonnoy,
407 J. B. R. Matthews, T. K. Maycock, T. Waterfield, O. Yelekçi, R. Yu, & B. Zhou, Eds.;
408 pp. 3–32). Cambridge University Press. <https://centaur.reading.ac.uk/101317/>
- 409 Angilletta, M. J. (2006). Estimating and comparing thermal performance curves. *Journal of*
410 *Thermal Biology*, 31(7), 541–545. <https://doi.org/10.1016/j.jtherbio.2006.06.002>
- 411 Angilletta, M. J. (2009). *Thermal Adaptation: A Theoretical and Empirical Synthesis*. OUP
412 Oxford.
- 413 Angilletta, M. J., Huey, R. B., & Frazier, M. R. (2010). Thermodynamic Effects on Organismal
414 Performance: Is Hotter Better? *Physiological and Biochemical Zoology*, 83(2), 197–206.
415 <https://doi.org/10.1086/648567>
- 416 Barrett, R. D. H., & Schluter, D. (2008). Adaptation from standing genetic variation. *Trends in*
417 *Ecology & Evolution*, 23(1), 38–44. <https://doi.org/10.1016/j.tree.2007.09.008>
- 418 Bathiany, S., Dakos, V., Scheffer, M., & Lenton, T. M. (2018). Climate models predict
419 increasing temperature variability in poor countries. *Science Advances*.
420 <https://doi.org/10.1126/sciadv.aar5809>

421 Bellard, C., Bertelsmeier, C., Leadley, P., Thuiller, W., & Courchamp, F. (2012). Impacts of
422 climate change on the future of biodiversity. *Ecology Letters*, *15*(4), 365–377.
423 <https://doi.org/10.1111/j.1461-0248.2011.01736.x>

424 Bennett, A. F., Lenski, R. E., & Mittler, J. E. (1992). Evolutionary Adaptation to Temperature. I.
425 Fitness Responses of Escherichia Coli to Changes in Its Thermal Environment.
426 *Evolution*, *46*(1), 16–30. <https://doi.org/10.1111/j.1558-5646.1992.tb01981.x>

427 Berger, D., Walters, R. J., & Blanckenhorn, W. U. (2014). Experimental evolution for generalists
428 and specialists reveals multivariate genetic constraints on thermal reaction norms.
429 *Journal of Evolutionary Biology*, *27*(9), 1975–1989. <https://doi.org/10.1111/jeb.12452>

430 Booth, D. J., Bond, N., Macreadie, P., Booth, D. J., Bond, N., & Macreadie, P. (2011). Detecting
431 range shifts among Australian fishes in response to climate change. *Marine and*
432 *Freshwater Research*, *62*(9), 1027–1042. <https://doi.org/10.1071/MF10270>

433 Buckley, L. B., Ehrenberger, J. C., & Angilletta, M. J. (2015). Thermoregulatory behaviour
434 limits local adaptation of thermal niches and confers sensitivity to climate change.
435 *Functional Ecology*, *29*(8), 1038–1047.

436 Burke, M. K., Liti, G., & Long, A. D. (2014). Standing Genetic Variation Drives Repeatable
437 Experimental Evolution in Outcrossing Populations of *Saccharomyces cerevisiae*.
438 *Molecular Biology and Evolution*, *31*(12), 3228–3239.
439 <https://doi.org/10.1093/molbev/msu256>

440 Chaturvedi, A., Zhou, J., Raeymaekers, J. A. M., Czypionka, T., Orsini, L., Jackson, C. E.,
441 Spanier, K. I., Shaw, J. R., Colbourne, J. K., & De Meester, L. (2021). Extensive standing
442 genetic variation from a small number of founders enables rapid adaptation in *Daphnia*.
443 *Nature Communications*, *12*(1), 4306. <https://doi.org/10.1038/s41467-021-24581-z>

444 Chevin, L.-M. (2013). Genetic Constraints on Adaptation to a Changing Environment. *Evolution*,
445 67(3), 708–721. <https://doi.org/10.1111/j.1558-5646.2012.01809.x>

446 Chevin, L.-M., Collins, S., & Lefèvre, F. (2013). Phenotypic plasticity and evolutionary
447 demographic responses to climate change: Taking theory out to the field. *Functional*
448 *Ecology*, 27(4), 967–979. <https://doi.org/10.1111/j.1365-2435.2012.02043.x>

449 Clusella-Trullas, S., Blackburn, T. M., & Chown, S. L. (2011). Climatic Predictors of
450 Temperature Performance Curve Parameters in Ectotherms Imply Complex Responses to
451 Climate Change. *The American Naturalist*, 177(6), 738–751.
452 <https://doi.org/10.1086/660021>

453 Condon, C., Acharya, A., Adrian, G. J., Hurliman, A. M., Malekooti, D., Nguyen, P., Zelic, M.
454 H., & Angilletta Jr, M. J. (2015). Indirect selection of thermal tolerance during
455 experimental evolution of *Drosophila melanogaster*. *Ecology and Evolution*, 5(9), 1873–
456 1880. <https://doi.org/10.1002/ece3.1472>

457 Cox, R. M., & Calsbeek, R. (2014). Survival of the fattest? Indices of body condition do not
458 predict viability in the brown anole (*Anolis sagrei*). *Functional Ecology*, 29(3), 404–413.
459 <https://doi.org/10.1111/1365-2435.12346>

460 Deutsch, C. A., Tewksbury, J. J., Huey, R. B., Sheldon, K. S., Ghalambor, C. K., Haak, D. C., &
461 Martin, P. R. (2008). Impacts of climate warming on terrestrial ectotherms across
462 latitude. *Proceedings of the National Academy of Sciences*, 105(18), 6668–6672.
463 <https://doi.org/10.1073/pnas.0709472105>

464 Elmhagen, B., Kindberg, J., Hellström, P., & Angerbjörn, A. (2015). A boreal invasion in
465 response to climate change? Range shifts and community effects in the borderland

466 between forest and tundra. *AMBIO*, 44(1), 39–50. <https://doi.org/10.1007/s13280-014->
467 0606-8

468 Fey, S. B., Vasseur, D. A., Alujević, K., Kroeker, K. J., Logan, M. L., O’Connor, M. I., Rudolf,
469 V. H. W., DeLong, J. P., Peacor, S., Selden, R. L., Sih, A., & Clusella-Trullas, S. (2019).
470 Opportunities for behavioral rescue under rapid environmental change. *Global Change*
471 *Biology*, 25(9), 3110–3120. <https://doi.org/10.1111/gcb.14712>

472 Fisher, R. A. (1958). *The genetical theory of natural selection*. Рипол Классик.

473 Fox, R. J., Donelson, J. M., Schunter, C., Ravasi, T., & Gaitán-Espitia, J. D. (2019). Beyond
474 buying time: The role of plasticity in phenotypic adaptation to rapid environmental
475 change. *Philosophical Transactions of the Royal Society B: Biological Sciences*,
476 374(1768), 20180174. <https://doi.org/10.1098/rstb.2018.0174>

477 Frankham, R. (1996). Relationship of Genetic Variation to Population Size in Wildlife.
478 *Conservation Biology*, 10(6), 1500–1508. <https://doi.org/10.1046/j.1523->
479 1739.1996.10061500.x

480 Gilchrist, G. W. (1995). Specialists and Generalists in Changing Environments. I. Fitness
481 Landscapes of Thermal Sensitivity. *The American Naturalist*, 146(2), 252–270.
482 <https://doi.org/10.1086/285797>

483 Gilchrist, G. W. (1996). A Quantitative Genetic Analysis of Thermal Sensitivity in the
484 Locomotor Performance Curve of *Aphidius Ervi*. *Evolution*, 50(4), 1560–1572.
485 <https://doi.org/10.1111/j.1558-5646.1996.tb03928.x>

486 Gilchrist, G. W., Huey, R. B., & Partridge, L. (1997). Thermal Sensitivity of *Drosophila*
487 *melanogaster*: Evolutionary Responses of Adults and Eggs to Laboratory Natural

488 Selection at Different Temperatures. *Physiological Zoology*, 70(4), 403–414.
489 <https://doi.org/10.1086/515853>

490 Grant, P. R., & Grant, B. R. (2002). Unpredictable Evolution in a 30-Year Study of Darwin's
491 Finches. *Science*. <https://doi.org/10.1126/science.1070315>

492 Hairston, N. G., Ellner, S. P., Geber, M. A., Yoshida, T., & Fox, J. A. (2005). Rapid evolution
493 and the convergence of ecological and evolutionary time. *Ecology Letters*, 8(10), 1114–
494 1127. <https://doi.org/10.1111/j.1461-0248.2005.00812.x>

495 Hochachka, P. W., & Somero, G. N. (2002). *Biochemical Adaptation: Mechanism and Process*
496 *in Physiological Evolution*. Oxford University Press.

497 Hoffmann, A. A., & Sgrò, C. M. (2011). Climate change and evolutionary adaptation. *Nature*,
498 470(7335), 479–485. <https://doi.org/10.1038/nature09670>

499 Huey, R. B., Hertz, P. E., & Sinervo, B. (2003). Behavioral Drive versus Behavioral Inertia in
500 Evolution: A Null Model Approach. *The American Naturalist*, 161(3), 357–366.
501 <https://doi.org/10.1086/346135>

502 Huey, R. B., & Stevenson, R. D. (1979). Integrating Thermal Physiology and Ecology of
503 Ectotherms: A Discussion of Approaches. *American Zoologist*, 19(1), 357–366.
504 <https://doi.org/10.1093/icb/19.1.357>

505 Izem, R., & Kingsolver, J. G. (2005). Variation in Continuous Reaction Norms: Quantifying
506 Directions of Biological Interest. *The American Naturalist*, 166(2), 277–289.
507 <https://doi.org/10.1086/431314>

508 Kearney, M., Shine, R., & Porter, W. P. (2009). The potential for behavioral thermoregulation to
509 buffer “cold-blooded” animals against climate warming. *Proceedings of the National*
510 *Academy of Sciences*, 106(10), 3835–3840. <https://doi.org/10.1073/pnas.0808913106>

511 Kingsolver, J. G., & Diamond, S. E. (2015). Phenotypic Selection in Natural Populations: What
512 Limits Directional Selection? *The American Naturalist*. <https://doi.org/10.1086/658341>

513 Kingsolver, J. G., Heckman, N., Zhang, J., Carter, P. A., Knies, J. L., Stinchcombe, J. R., &
514 Meyer, K. (2015). Genetic Variation, Simplicity, and Evolutionary Constraints for
515 Function-Valued Traits. *The American Naturalist*, *185*(6), E166–E181.
516 <https://doi.org/10.1086/681083>

517 Kingsolver, J. G., Ragland, G. J., & Shlichta, J. G. (2004). Quantitative Genetics of Continuous
518 Reaction Norms: Thermal Sensitivity of Caterpillar Growth Rates. *Evolution*, *58*(7),
519 1521–1529. <https://doi.org/10.1111/j.0014-3820.2004.tb01732.x>

520 Knies, J. L., Izem, R., Supler, K. L., Kingsolver, J. G., & Burch, C. L. (2006). The Genetic Basis
521 of Thermal Reaction Norm Evolution in Lab and Natural Phage Populations. *PLOS*
522 *Biology*, *4*(7), e201. <https://doi.org/10.1371/journal.pbio.0040201>

523 Knies, J. L., Kingsolver, J. G., & Burch, C. L. (2009). Hotter Is Better and Broader: Thermal
524 Sensitivity of Fitness in a Population of Bacteriophages. *The American Naturalist*,
525 *173*(4), 419–430. <https://doi.org/10.1086/597224>

526 Lande, R. (1993). Risks of Population Extinction from Demographic and Environmental
527 Stochasticity and Random Catastrophes. *The American Naturalist*, *142*(6), 911–927.
528 <https://doi.org/10.1086/285580>

529 Latimer, C. a. L., Wilson, R. S., & Chenoweth, S. F. (2011). Quantitative genetic variation for
530 thermal performance curves within and among natural populations of *Drosophila serrata*.
531 *Journal of Evolutionary Biology*, *24*(5), 965–975. [https://doi.org/10.1111/j.1420-](https://doi.org/10.1111/j.1420-9101.2011.02227.x)
532 [9101.2011.02227.x](https://doi.org/10.1111/j.1420-9101.2011.02227.x)

533 Logan, M. L., & Cox, C. L. (2020). Genetic Constraints, Transcriptome Plasticity, and the
534 Evolutionary Response to Climate Change. *Frontiers in Genetics, 0*.
535 <https://doi.org/10.3389/fgene.2020.538226>

536 Logan, M. L., Cox, R. M., & Calsbeek, R. (2014). Natural selection on thermal performance in a
537 novel thermal environment. *Proceedings of the National Academy of Sciences, 111*(39),
538 14165–14169. <https://doi.org/10.1073/pnas.1404885111>

539 Logan, M. L., Curlis, J. D., Gilbert, A. L., Miles, D. B., Chung, A. K., McGlothlin, J. W., & Cox,
540 R. M. (2018). Thermal physiology and thermoregulatory behaviour exhibit low
541 heritability despite genetic divergence between lizard populations. *Proceedings of the*
542 *Royal Society B: Biological Sciences*. <https://doi.org/10.1098/rspb.2018.0697>

543 Logan, M. L., Minnaar, I. A., Keegan, K. M., & Clusella-Trullas, S. (2020). The evolutionary
544 potential of an insect invader under climate change*. *Evolution, 74*(1), 132–144.
545 <https://doi.org/10.1111/evo.13862>

546 Logan, M. L., Neel, L. K., Nicholson, D. J., Stokes, A. J., Miller, C. L., Chung, A. K., Curlis, J.
547 D., Keegan, K. M., Rosso, A. A., Maayan, I., Folfas, E., Williams, C. E., Casement, B.,
548 Gallegos Koyner, M. A., Padilla Perez, D. J., Falvey, C. H., Alexander, S. M., Charles,
549 K. L., Graham, Z. A., ... Cox, C. L. (2021). Sex-specific microhabitat use is associated
550 with sex-biased thermal physiology in Anolis lizards. *Journal of Experimental Biology,*
551 *224*(2). <https://doi.org/10.1242/jeb.235697>

552 Logan, M. L., van Berkel, J., & Clusella-Trullas, S. (2019). The Bogert Effect and environmental
553 heterogeneity. *Oecologia, 191*(4), 817–827. <https://doi.org/10.1007/s00442-019-04541-7>

554 Losos, J. B. (2011). *Lizards in an Evolutionary Tree: Ecology and Adaptive Radiation of Anoles*.
555 Univ of California Press.

556 Martins, F., Kruuk, L., Llewelyn, J., Moritz, C., & Phillips, B. (2019). Heritability of climate-
557 relevant traits in a rainforest skink. *Heredity*, *122*(1), 41–52.
558 <https://doi.org/10.1038/s41437-018-0085-y>

559 Muñoz, M. M. (2022). The Bogert effect, a factor in evolution. *Evolution*, *76*(S1), 49–66.
560 <https://doi.org/10.1111/evo.14388>

561 Neel, L. K., Logan, M. L., Nicholson, D. J., Miller, C., Chung, A. K., Maayan, I., Degon, Z.,
562 DuBois, M., Curlis, J. D., Taylor, Q., Keegan, K. M., McMillan, W. O., Losos, J. B., &
563 Cox, C. L. (2021). Habitat structure mediates vulnerability to climate change through its
564 effects on thermoregulatory behavior. *Biotropica*, *53*(4), 1121–1133.
565 <https://doi.org/10.1111/btp.12951>

566 O’Grady, J. J., Reed, D. H., Brook, B. W., & Frankham, R. (2004). What are the best correlates
567 of predicted extinction risk? *Biological Conservation*, *118*(4), 513–520.
568 <https://doi.org/10.1016/j.biocon.2003.10.002>

569 Padmavathi, C., Katti, G., Sailaja, V., Padmakumari, A. P., Jhansilakshmi, V., Prabhakar, M., &
570 Prasad, Y. G. (2013). Temperature Thresholds and Thermal Requirements for the
571 Development of the Rice Leaf Folder, *Cnaphalocrocis medinalis*. *Journal of Insect*
572 *Science*, *13*, 96. <https://doi.org/10.1673/031.013.9601>

573 Phillips, B. L., Llewelyn, J., Hatcher, A., Macdonald, S., & Moritz, C. (2014). Do evolutionary
574 constraints on thermal performance manifest at different organizational scales? *Journal of*
575 *Evolutionary Biology*, *27*(12), 2687–2694. <https://doi.org/10.1111/jeb.12526>

576 Richter-Boix, A., Katzenberger, M., Duarte, H., Quintela, M., Tejedo, M., & Laurila, A. (2015).
577 Local divergence of thermal reaction norms among amphibian populations is affected by

578 pond temperature variation. *Evolution*, 69(8), 2210–2226.
579 <https://doi.org/10.1111/evo.12711>

580 Roff, D. A., & Fairbairn, D. J. (2012). A Test of the Hypothesis That Correlational Selection
581 Generates Genetic Correlations. *Evolution*, 66(9), 2953–2960.
582 <https://doi.org/10.1111/j.1558-5646.2012.01656.x>

583 Schlötterer, C., Kofler, R., Versace, E., Tobler, R., & Franssen, S. U. (2015). Combining
584 experimental evolution with next-generation sequencing: A powerful tool to study
585 adaptation from standing genetic variation. *Heredity*, 114(5), 431–440.
586 <https://doi.org/10.1038/hdy.2014.86>

587 Schou, M. F., Engelbrecht, A., Brand, Z., Svensson, E. I., Cloete, S., & Cornwallis, C. K. (2022).
588 Evolutionary trade-offs between heat and cold tolerance limit responses to fluctuating
589 climates. *Science Advances*. <https://doi.org/10.1126/sciadv.abn9580>

590 Sears, M. W., & Angilletta, M. J. (2015). Costs and Benefits of Thermoregulation Revisited:
591 Both the Heterogeneity and Spatial Structure of Temperature Drive Energetic Costs. *The*
592 *American Naturalist*, 185(4), E94–E102. <https://doi.org/10.1086/680008>

593 Sears, M. W., Angilletta, M. J., Schuler, M. S., Borchert, J., Dilliplane, K. F., Stegman, M.,
594 Rusch, T. W., & Mitchell, W. A. (2016). Configuration of the thermal landscape
595 determines thermoregulatory performance of ectotherms. *Proceedings of the National*
596 *Academy of Sciences*, 113(38), 10595–10600. <https://doi.org/10.1073/pnas.1604824113>

597 Sinervo, B., Méndez-de-la-Cruz, F., Miles, D. B., Heulin, B., Bastiaans, E., Cruz, M. V.-S.,
598 Lara-Resendiz, R., Martínez-Méndez, N., Calderón-Espinosa, M. L., Meza-Lázaro, R. N.,
599 Gadsden, H., Avila, L. J., Morando, M., Riva, I. J. D. la, Sepulveda, P. V., Rocha, C. F.
600 D., Ibarngüengoytía, N., Puntriano, C. A., Massot, M., ... Jack W. Sites, J. (2010). Erosion

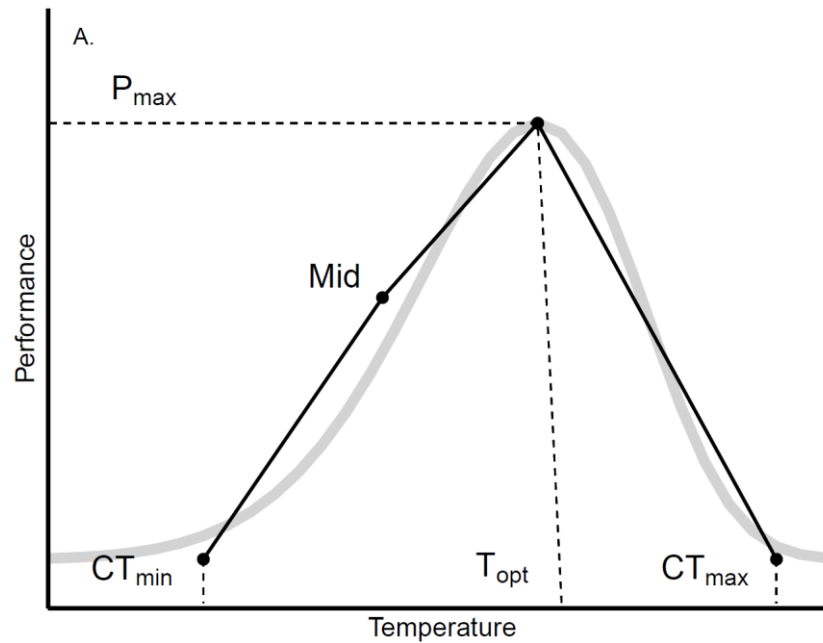
601 of Lizard Diversity by Climate Change and Altered Thermal Niches. *Science*.
602 <https://doi.org/10.1126/science.1184695>

603 Teotónio, H., Chelo, I. M., Bradić, M., Rose, M. R., & Long, A. D. (2009). Experimental
604 evolution reveals natural selection on standing genetic variation. *Nature Genetics*, *41*(2),
605 251–257. <https://doi.org/10.1038/ng.289>

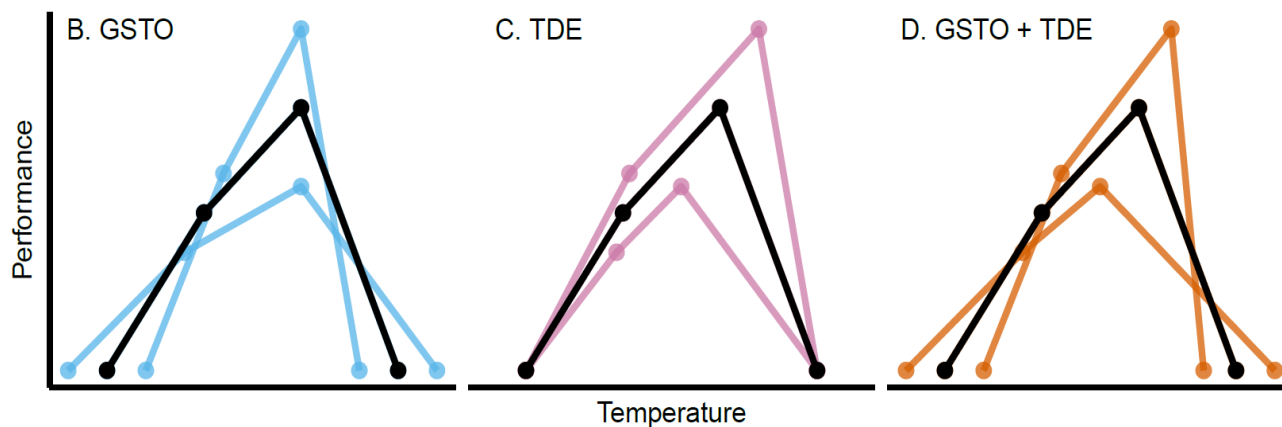
606 van Berkum, F. H. (1986). Evolutionary Patterns of the Thermal Sensitivity of Sprint Speed in
607 Anolis Lizards. *Evolution*, *40*(3), 594–604. [https://doi.org/10.1111/j.1558-
608 5646.1986.tb00510.x](https://doi.org/10.1111/j.1558-5646.1986.tb00510.x)

609 Vasseur, D. A., DeLong, J. P., Gilbert, B., Greig, H. S., Harley, C. D. G., McCann, K. S.,
610 Savage, V., Tunney, T. D., & O'Connor, M. I. (2014). Increased temperature variation
611 poses a greater risk to species than climate warming. *Proceedings of the Royal Society B:
612 Biological Sciences*. <https://doi.org/10.1098/rspb.2013.2612>

613
614
615
616
617
618
619
620
621
622
623



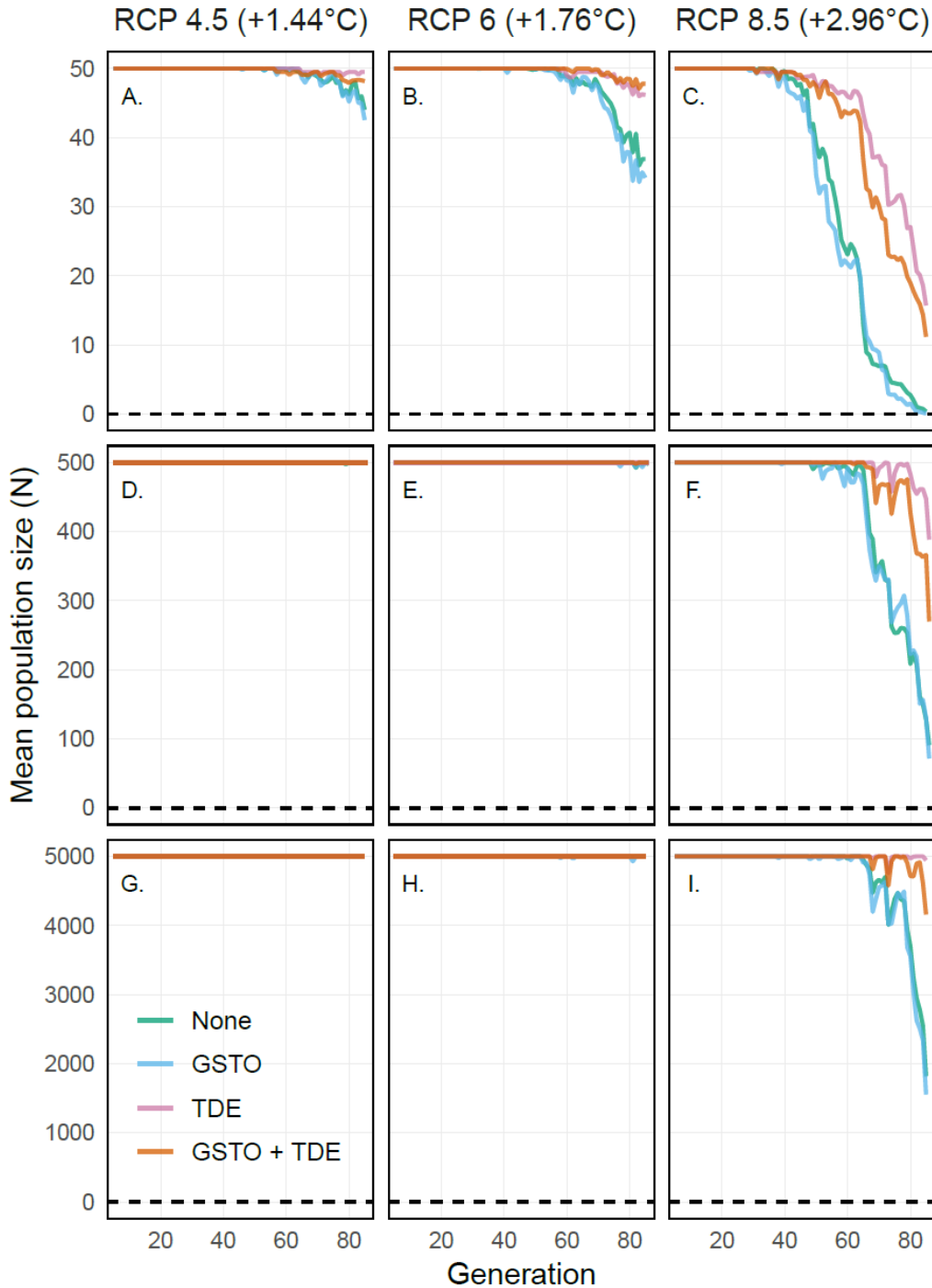
625



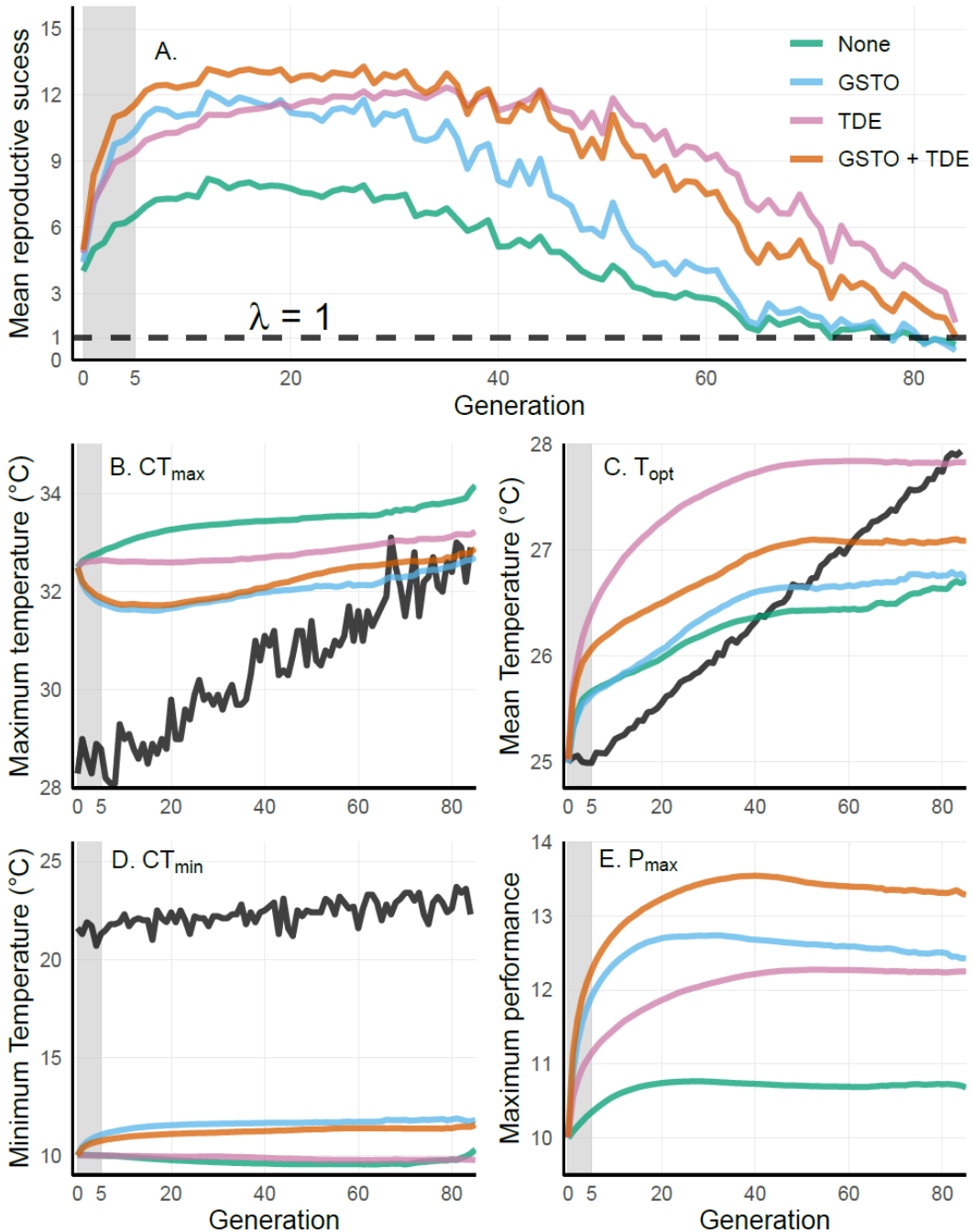
626

627 **Figure 1.** The general structure of thermal performance curves (TPCs) and genetic correlations
 628 in our simulations. (a) We used a minimum convex polygon approach (black polygon) to
 629 approximate a traditional non-linear TPC function (gray curve). (b-d) Phenotypic variability in
 630 TPC shapes under the generalist-specialist trade-off (GSTO, b), the thermodynamic effect (TDE,
 631 c) and both the GSTO and the TDE simultaneously (GSTO + TDE, d). For panels b-d, black
 632 TPC polygons indicate population averages while colored polygons indicate extreme
 633 phenotypes.

634



635
 636 **Figure 2.** Changes in average population size over 80 generations (80 years) of environmental
 637 change. Populations were exposed to three different climate change scenarios (columns) and
 638 starting population sizes (rows). For each pairwise combination of starting population size and
 639 climate change scenario, we modeled changes in population size for populations whose TPC
 640 shapes were unconstrained by genetic correlations (None, green lines), or constrained by a
 641 generalist-specialist trade-off (GSTO, blue lines), a thermodynamic effect (TDE, purple lines), or
 642 both a generalist-specialist trade-off and a thermodynamic effect (GSTO + TDE, orange lines).
 643 In all cases, lines indicate the mean population size (N) for 100 simulation replicates.



644
 645
 646
 647
 648
 649
 650
 651
 652
 653
 654

Figure 3. Mean reproductive success (A) and evolutionary change in thermal performance traits (B-E) with respect to changes in the thermal environment across all $N_0 = 500$ populations exposed to the RCP 8.5 climate change scenario. For all panels, colored lines indicate the genetic correlation populations were subjected to and correspond to the mean across 100 simulation replicates. “None” indicates unconstrained populations (green), “GSTO” indicates populations subjected to the generalist-specialist trade-off (blue), “TDE” indicates populations subject to the thermodynamic effect (purple) and “GSTO + TDE” indicates populations subjected to both the generalist-specialist trade-off and thermodynamic effect (orange). The shaded areas indicate the burn-in period (generations 0-5) where no environmental change occurred. For panel A, the

655 black dashed line indicates a mean reproductive success of 1 ($\lambda = 1$), above which a population
656 would grow and below which it would decline. For panels B-D, black lines indicate the
657 maximum (B), mean (C) and minimum (D) environmental temperatures experienced each
658 generation while colored lines indicate changes in CT_{max} (B), T_{opt} (C), CT_{min} (D), and P_{max} (E).

659
660
661
662
663
664
665
666
667
668
669
670
671
672
673
674
675
676
677
678
679
680
681
682
683
684
685
686
687
688
689
690
691
692
693
694
695

696 **Supplementary Materials**

697

698 **1. Methodological Details**

699

700 **Generating starting populations**

701 Each starting population was composed of a set of unique TPCs. To construct these TPCs, we
702 used four baseline ‘thermal performance traits’ which are commonly used to describe TPCs in
703 empirical studies (and thus their evolution is easily interpretable; Logan et al., 2014; Logan &
704 Cox, 2020). These traits were the thermal optimum (T_{opt}), the critical thermal limits (CT_{min} &
705 CT_{max}), maximum performance (P_{max}), and an intermediate temperature point (which we term
706 “Mid”) between CT_{min} and T_{opt} to allow for the stereotypical left skewness of TPCs (Angilletta,
707 2006). We chose a set of base values for each of these traits ($T_{opt} = 25^{\circ} C$, $CT_{min} = 10^{\circ} C$, CT_{max}
708 $= 35^{\circ} C$, $P_{max} = 10$) with “Mid” being at a temperature value of $19^{\circ}C$ (halfway between the base
709 values of CT_{min} and T_{opt}) and a performance value of 5 (the P_{max} base value divided by two). The
710 specific base values are arbitrary and not crucial for interpreting the role of genetic correlations
711 (see below), although we chose these values because they are similar to what has been measured
712 in real populations of mid-latitude ectotherms (e.g. Padmavathi et al., 2013). To generate among-
713 individual variation in TPC shapes within each starting population, we randomized the base
714 values using the following formula:

715

$$Randomized\ Trait = Base\ Trait + QG \quad (1)$$

$$Q \sim N(0,1) \quad (2)$$

716

717 Whereby a base value would be modified by adding a quantity (Q) sampled from a normal
718 distribution of mean = 0 and standard deviation = 1, and then multiplied by a genetic variance-

719 covariance matrix (G) to obtain the randomized value. We used a different G -matrix to generate
 720 populations according to each genetic correlation scenario. For populations governed by only a
 721 GSTO, we used the following G :

722

$$G_{GSTO} = \begin{bmatrix} CT_{min} & Mid & T_{opt} & CT_{max} & P_{max} \\ 1 & 0 & 0 & 0 & 0.75 \\ 0 & 1 & 0 & 0 & 0.75 \\ 0 & 0 & 1 & 0 & 0 \\ 0 & 0 & 0 & 1 & -0.75 \\ 0.75 & 0.75 & 0 & -0.75 & 1 \end{bmatrix} \begin{matrix} CT_{min} \\ Mid \\ T_{opt} \\ CT_{max} \\ P_{max} \end{matrix} \quad (3)$$

723

724 This matrix included a positive correlation between P_{max} and both CT_{min} and Mid , and a negative
 725 correlation between P_{max} and CT_{max} , because a GSTO should result in reduced maximal
 726 performance capacity when performance increases at or near the tolerance limits. Here and
 727 below, we used a genetic correlation strength of 0.75 (or -0.75) such that correlations were strong
 728 but not overwhelmingly so. For populations governed by only the TDE, we used the following
 729 G :

730

$$G_{TDE} = \begin{bmatrix} CT_{min} & Mid & T_{opt} & CT_{max} & P_{max} \\ 1 & 0 & 0 & 0 & 0 \\ 0 & 1 & 0 & 0 & 0 \\ 0 & 0 & 1 & 0 & 0.75 \\ 0 & 0 & 0 & 1 & 0 \\ 0 & 0 & 0.75 & 0 & 1 \end{bmatrix} \begin{matrix} CT_{min} \\ Mid \\ T_{opt} \\ CT_{max} \\ P_{max} \end{matrix} \quad (4)$$

731

732 This matrix included a positive correlation between T_{opt} and P_{max} , but no other correlations,
 733 because this is the sole relationship among thermal performance traits that defines the TDE. For
 734 populations governed by both a GSTO and a TDE, we used the following G :

735

$$G_{GSTO+TDE} = \begin{matrix} & \begin{matrix} CT_{min} & Mid & T_{opt} & CT_{max} & P_{max} \end{matrix} \\ \begin{bmatrix} 1 & 0 & 0 & 0 & 0.75 \\ 0 & 1 & 0 & 0 & 0.75 \\ 0 & 0 & 1 & 0 & 0.75 \\ 0 & 0 & 0 & 1 & -0.75 \\ 0.75 & 0.75 & 0.75 & -0.75 & 1 \end{bmatrix} & \begin{matrix} CT_{min} \\ Mid \\ T_{opt} \\ CT_{max} \\ P_{max} \end{matrix} \end{matrix} \quad (5)$$

736

737 This matrix included all pairwise genetic correlations that are expected when both a GSTO and a
 738 TDE are present in the same population. Finally, for populations whose TPC shapes were not
 739 constrained by genetic correlations, G was defined as a 5×5 identity matrix with all correlations
 740 among traits set to zero.

741 After obtaining the final set of trait values defining an individual's TPC, we removed or
 742 corrected any values that would result in TPCs with impossible shapes. For example, we
 743 corrected instances in which the trait randomization or the multiplication by G had resulted in
 744 individuals with $CT_{min} > T_{opt}$ or $CT_{max} < T_{opt}$. After removal of these individuals, the remaining
 745 values were used as the basis to generate a unique TPC for each individual. We used a simple
 746 minimum convex polygon algorithm to construct TPCs from trait values (Angilletta, 2009; van
 747 Berkum, 1986). We built TPCs by linearly connecting adjacent trait values to form a polygon
 748 that approximated the shape of the curve (Figure 1A). As opposed to curve-fitting (an alternative
 749 approach used in empirical studies, e.g. Angilletta, 2006), this procedure ensured that the genetic
 750 correlations specified in G would be perfectly represented in the trait distribution of each starting

751 population because there were no parameters with pre-existing correlation structures (as would
752 often be the case when curve fitting; Figure S2). For each combination of genetic correlation
753 scenario and starting population size (4 x 3), we generated 10 unique populations (based on the
754 same G) to avoid the possibility of drawing general conclusions from a single anomalous starting
755 trait distribution.

756

757 **Simulating thermal environments**

758 For all simulations, we set the initial environmental conditions to a mean daily environmental
759 temperature (T_m) of 25 °C and a standard deviation (T_{sd}) of 1 °C. Thus, all populations started
760 out in a relatively stable thermal environment that closely matched the characteristics of their
761 TPCs (i.e., they were locally adapted). We simulated climate change following the RCP 4.5
762 ($\Delta T_m = 1.44$ °C), RCP 6 ($\Delta T_m = 1.76$ °C), and RCP 8.5 ($\Delta T_m = 2.96$ °C) IPCC scenarios through
763 the year 2100. For all IPCC scenarios, we assumed a 15% increase in T_{sd} for every 1°C increase
764 in T_m following Bathinay et al. (2018). We also included a set of control simulations in which
765 thermal conditions did not change ($\Delta T_m = 0$ °C, $\Delta T_{sd} = 0$ °C). In addition to these three IPCC
766 scenarios and the control, we generated four more temperature change scenarios to tease apart
767 the effects of specific environmental and climate change features on population dynamics and
768 TPC evolution. For these, we used the RCP 8.5 scenario but kept either ΔT_m or ΔT_{sd} at zero
769 while allowing the other to change. We included additional RCP 8.5 simulations (again with
770 control simulations) but with double the initial T_{sd} (2°C) to explore the effects of a more variable
771 starting thermal environment on subsequent population dynamics and evolution.

772 To generate the specific thermal environments that a given population was exposed to
773 each generation, we first defined a sequence of 80 T_m and T_{sd} values (one for each year or

774 generation with a 5-year burn-in). These values increased linearly following the particular
775 climate change scenario being modeled. Within each generation, these base values were then
776 used to generate a normal distribution from which we sampled 150 daily temperatures. We chose
777 150 days to represent the breeding season of our hypothetical ectotherm, as this is similar to the
778 length of this period in some real species (e.g. Cox & Calsbeek, 2014), although the specific
779 length of the breeding season is unlikely to impact the results of simulations. For all simulations,
780 we introduced a “burn-in” period of five generations during which we did not allow the thermal
781 environment to change such that populations could further adapt to local conditions. For each
782 climate change scenario, we generated 10 unique sequences of temperature change (but from the
783 same starting environmental temperature distribution in each generation) to ensure that our
784 results were robust to anomalous years arising from the random sampling of the temperature
785 distribution in any given generation.

786

787 **Modeling survival and reproduction**

788 In our simulations, changes in population size ultimately arose from variation in the survival and
789 reproductive success of individuals, much as it would in real populations. For each day in a given
790 simulation, the performance of each individual was calculated by combining information about
791 the daily environmental temperature with individuals’ TPCs. Specifically, we calculated an
792 individual’s performance from its TPC and then used this performance value to generate a daily
793 survival probability according to the following expression:

794

$$P(S)_i = (1 + e^{-(\alpha + \beta p_i)})^{-1} \quad (6)$$

795

796 Where, for a given day (i) the probability of surviving ($P(S)_i$) is related to the individual's
797 performance (p_i) through a logistic function. In all cases, the values of the parameters α and β
798 were set to -5 and 1 respectively such that $P(S)_i = 0.5$ when $p_i = 5$, with the value of 5 being
799 a performance exactly half of the base value of P_{\max} . We then used each individual's $P(S)$ on a
800 particular day to calculate its actual survival (S) such that:

801

$$S_i \sim \text{Bernoulli}(P(S)_i) \quad (7)$$

802

803 This approach adds a stochastic component to survival which more closely mimics the dynamics
804 of real populations and produces a binary outcome of either death (0) or survival (1) for every
805 individual on every day of the simulation. After an individual reached a value of $S = 0$ for a
806 given day, it would be considered dead for all remaining days within that generation. We then
807 calculated reproductive success (R_g) of each individual as:

808

$$R_g = \left\lfloor \frac{1}{10} \sum_i^{150} S_i \right\rfloor \quad (8)$$

809

810 Whereby reproductive success within a generation (R_g) was an integer corresponding to 10% of
811 the rounded-down sum of all survived days within a generation. Since the number of days within
812 a generation was set at 150, the maximum possible reproductive output for any individual
813 through an entire generation was 15, and an individual had to survive at least 10 days in order to
814 produce one offspring. This simulation structure mimics the often empirically measured
815 “viability selection”, whereby longer survival over the breeding season is assumed to lead to

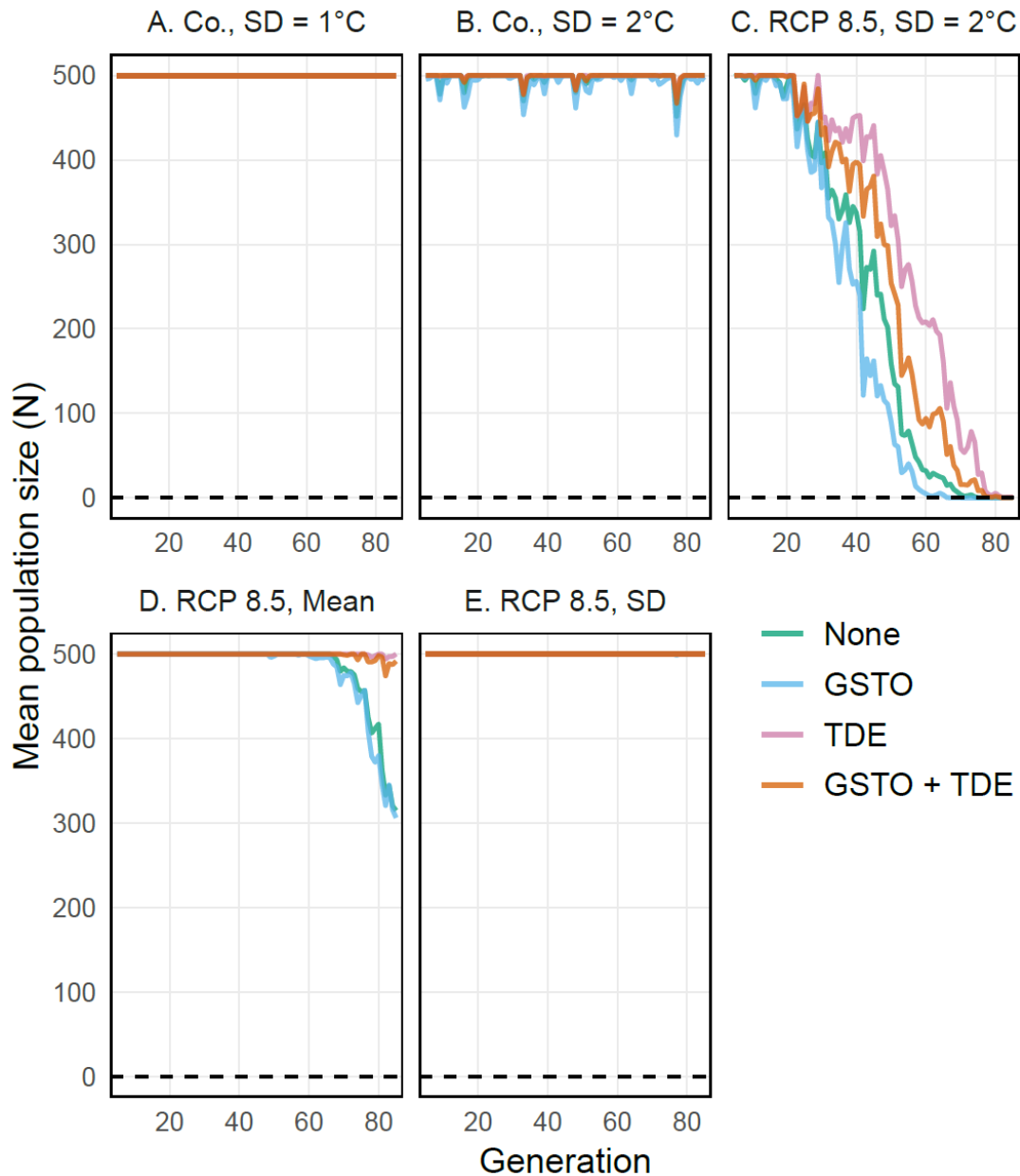
816 greater reproductive success and follows the breeding biology of some well-known vertebrate
817 groups such as *Anolis* lizards (Losos, 2011). Because individuals are represented solely by their
818 TPCs, offspring produced by an individual were assigned the exact same TPC as the parent (i.e.,
819 asexual cloning with a heritability of 1). Lastly, if the number of newly generated individuals
820 exceeded the initial population size (carrying capacity), a random sample of offspring that
821 equaled the carrying capacity was drawn to form the population for the next generation.

822 We ran unique simulations for every combination of genetic correlation and thermal
823 environment. For example, when exposing GSTO-constrained populations to the RCP 4.5
824 scenario, we ran a simulation exposing each of the 10 population replicates (based on same base
825 values but differing because of randomization around those values) to each of the 10 thermal
826 environment replicates (based on the same change in mean and standard deviation but differing
827 because of random sampling of the temperature distribution within each generation) for a total of
828 100 simulations. For each combination of genetic correlation and thermal environment,
829 population sizes and TPC characteristics were recorded as the average of the 100 simulations in
830 each generation. We did this for all 64 combinations presented in Tables S1 and S2 which totaled
831 6400 unique individual-based simulations.

832
833
834
835
836
837
838
839
840
841
842
843
844

845
846

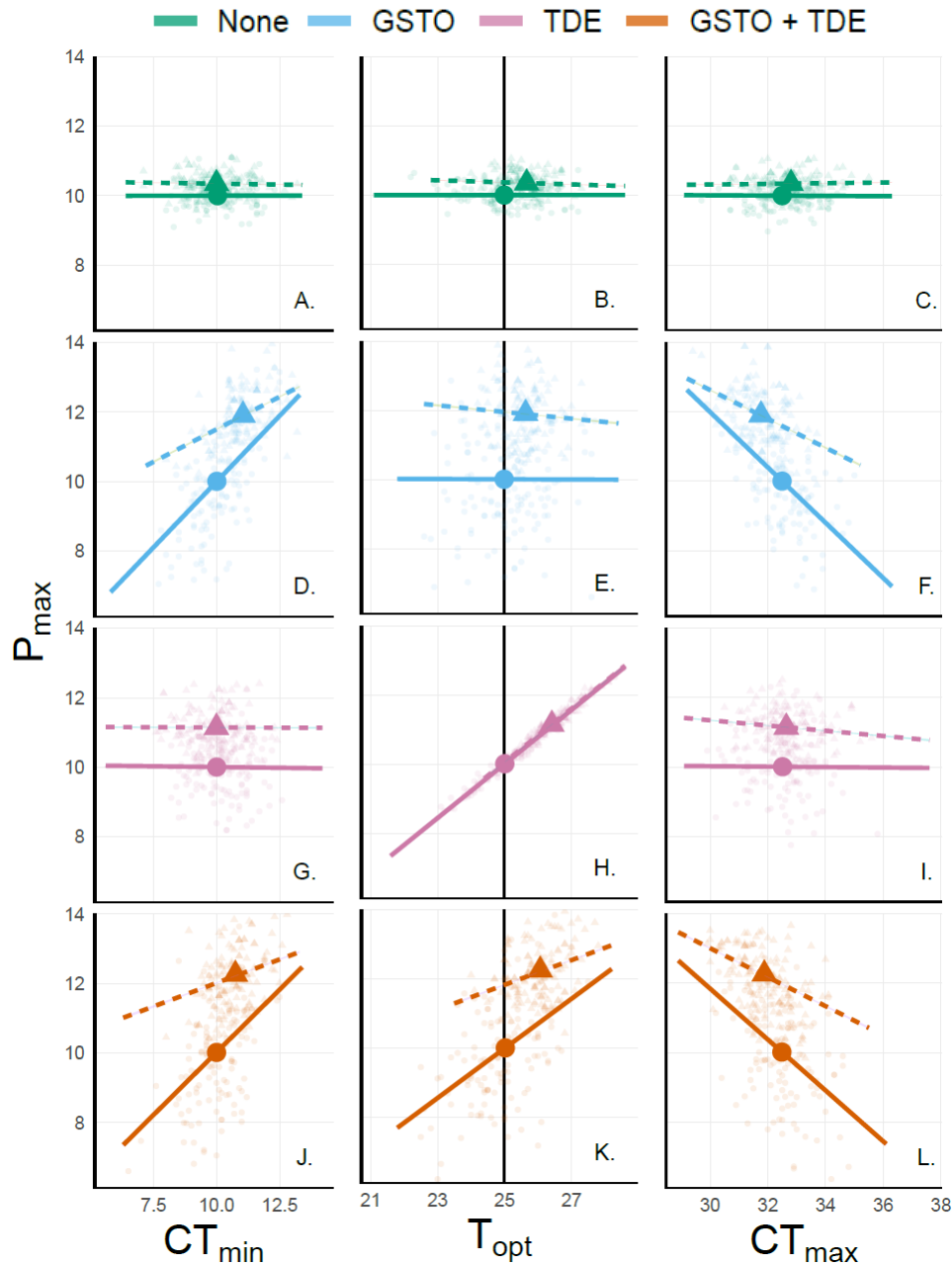
2. Supplementary Figures:



847

848 **Figure S1.** Changes in population size across different simulated conditions. Each panel
849 indicates the climate change scenario to which populations were exposed to; a control (Co.) with
850 no environmental change (with initial standard deviation (SD) in temperature of 1°C) (a), a
851 control with a more thermally variable environment (Initial SD = 2°C) (b), the RCP 8.5 climate
852 change scenario on an initially more variable thermal environment (+ 2.96°C in mean
853 temperature & Initial SD = 2°C) (c) and the RCP 8.5 scenario with only changes in mean daily
854 temperature (e) or standard deviation in temperature (f) with Initial SD = 1°C. Line color
855 indicates the genetic correlation to which populations were subject to. In all cases, N_0 & $K = 500$
856 and lines indicate the mean population size (N) for 100 simulation replicates.

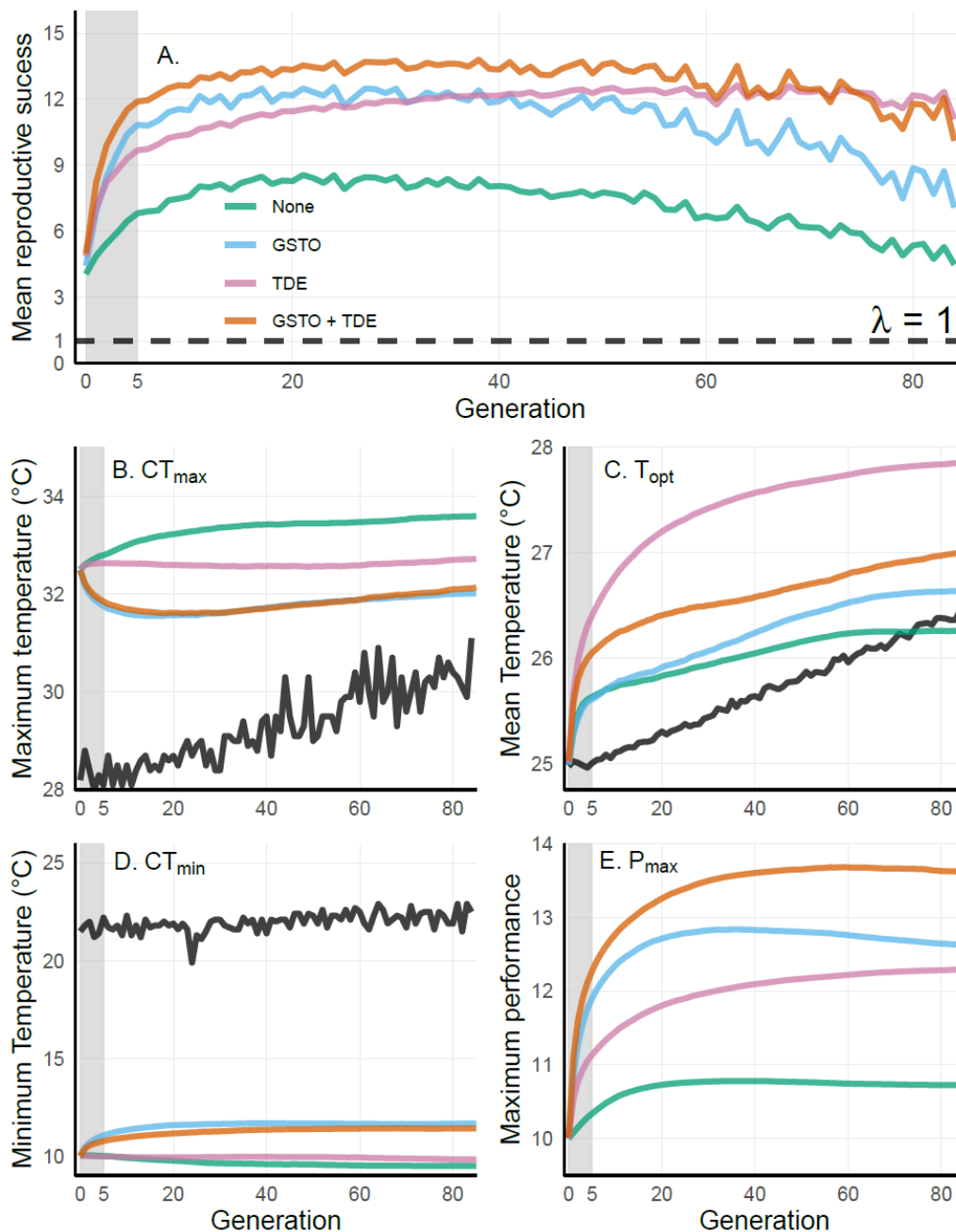
857



858

859

860 **Figure S2.** Relationship between P_{\max} and T_{opt} (left column) and P_{\max} and CT_{max} (right column,
 861 as a representative of TPC breath) in simulations where N_0 & $K = 500$ populations were exposed
 862 to the RCP 8.5 climate change scenario at the start (generation 0, solid line & circles) and the end
 863 of the acclimation period (generation 5, dashed line & triangles). Rows and color indicate the
 864 genetic correlation each population was subjected to. The solid point indicates the mean
 865 phenotype of the population, and the line indicates the distribution and range of phenotypes
 866 across the entire population. Light background points show a representative sample of
 867 phenotypic variability.
 868



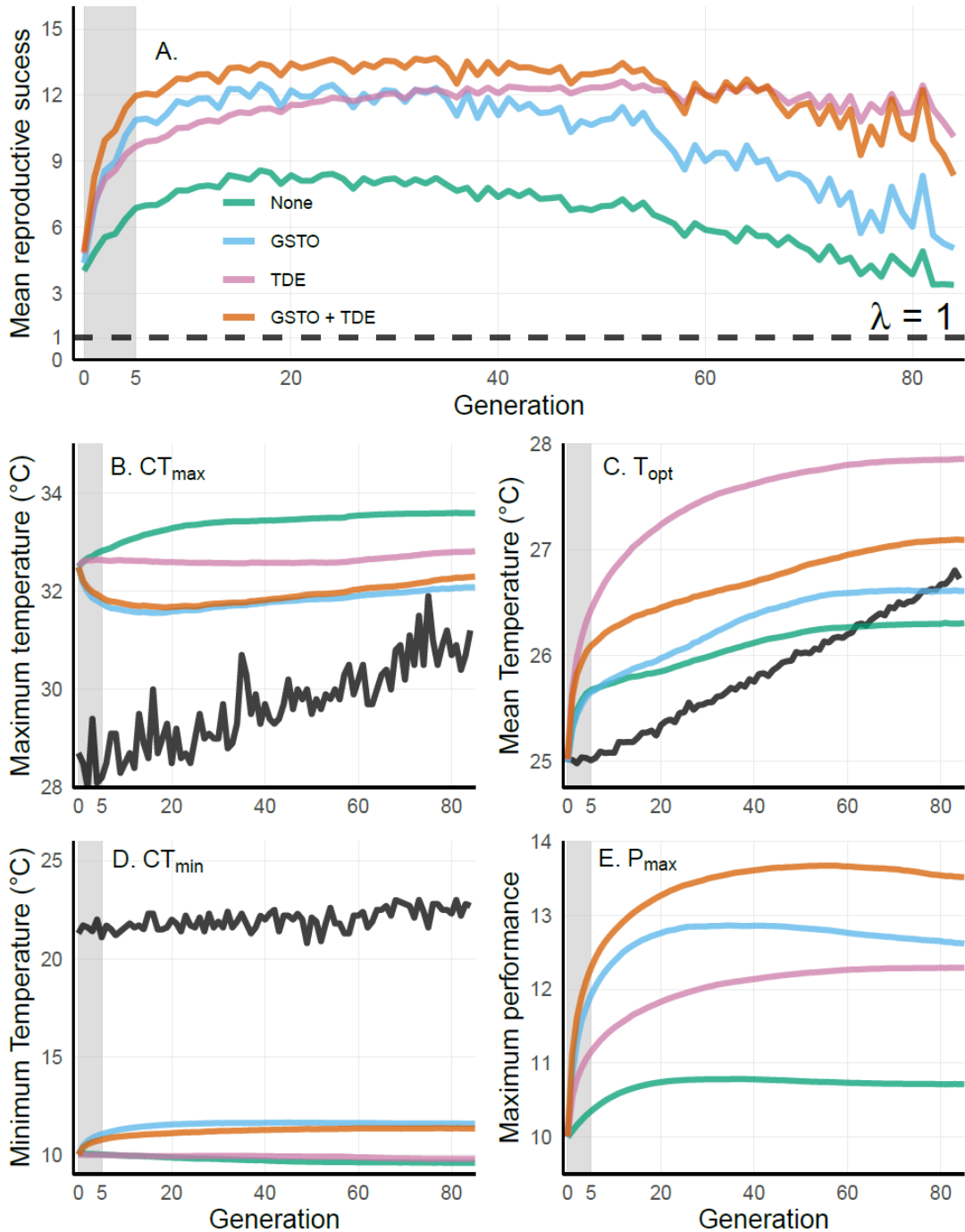
870

871

872 **Figure S3.** Mean reproductive success (A) and evolutionary change in thermal performance
 873 traits (B-E) with respect to changes in the thermal environment across all $N_0 = 500$ populations
 874 exposed to the RCP 4.5 climate change scenario. For all panels, colored lines indicate the genetic
 875 correlation populations were subjected to and correspond to the mean across 100 simulation
 876 replicates. “None” indicates unconstrained populations (green), “GSTO” indicates populations
 877 subjected to the generalist-specialist trade-off (blue), “TDE” indicates populations subject to the
 878 thermodynamic effect (purple) and “GSTO + TDE” indicates populations subjected to both the
 879 generalist-specialist trade-off and thermodynamic effect (orange). The shaded areas indicate the
 880 burn-in period (generations 0-5) where no environmental change occurred. For panel A, the

881 black dashed line indicates a mean reproductive success of 1 ($\lambda = 1$), above which a population
882 would grow and below which it would decline. For panels B-D, black lines indicate the
883 maximum (B), mean (C) and minimum (D) environmental temperatures experienced each
884 generation while colored lines indicate changes in CT_{\max} (B), T_{opt} (C), CT_{\min} (D), and P_{\max} (E).

885
886
887
888
889
890
891
892
893
894
895
896
897
898
899
900
901
902
903
904
905
906
907
908
909
910
911
912
913
914
915
916
917
918
919
920
921
922
923
924
925
926



927
928

929 **Figure S4.** Mean reproductive success (A) and evolutionary change in thermal performance
930 traits (B-E) with respect to changes in the thermal environment across all $N_0 = 500$ populations
931 exposed to the RCP 6 climate change scenario. For all panels, colored lines indicate the genetic
932 correlation populations were subjected to and correspond to the mean across 100 simulation
933 replicates. “None” indicates unconstrained populations (green), “GSTO” indicates populations
934 subjected to the generalist-specialist trade-off (blue), “TDE” indicates populations subject to the
935 thermodynamic effect (purple) and “GSTO + TDE” indicates populations subjected to both the

936 generalist-specialist trade-off and thermodynamic effect (orange). The shaded areas indicate the
937 burn-in period (generations 0-5) where no environmental change occurred. For panel A, the
938 black dashed line indicates a mean reproductive success of 1 ($\lambda = 1$), above which a population
939 would grow and below which it would decline. For panels B-D, black lines indicate the
940 maximum (B), mean (C) and minimum (D) environmental temperatures experienced each
941 generation while colored lines indicate changes in CT_{\max} (B), T_{opt} (C), CT_{\min} (D), and P_{\max} (E).

942
943
944
945
946
947
948
949
950
951
952
953
954
955
956
957
958
959
960
961
962
963
964
965
966
967
968
969
970
971
972
973
974
975
976

977 **3. Supplementary Tables**

978

979 **Table S1.** Population sizes and percentage of population decline across different simulated
 980 conditions based on IPCC climate change models.
 981

		Climate Change Scenario				$\overline{\text{RCP}}$	$\overline{\text{RCP}}$ per Genetic Correlation	
		Control	RCP 4.5	RCP 6	RCP 8.5			
Genetic Correlation	None	50	50 (0%)	44.04 (11.92%)	36.91 (26.18%)	0.35 (99.3%)	27.1 (45.8%)	32.56%
		500	500 (0%)	500 (0%)	497.92 (0.4%)	41.86 (91.63%)	346.59 (30.68%)	
		5000	5000 (0%)	5000 (0%)	5000 (0%)	1818.51 (63.62%)	3939.5 (21.21%)	
	GSTO	50	50 (0%)	42.55 (14.9%)	34.20 (31.6%)	0.07 (99.86%)	25.61 (48.79%)	34.54%
		500	500 (0%)	500 (0%)	499.53 (0.09%)	22.90 (95.42%)	340.81 (31.84%)	
		5000	5000 (0%)	5000 (0%)	5000 (0%)	1554.22 (68.92%)	3851.41 (22.97%)	
	TDE	50	50 (0%)	49.50 (1%)	46.18 (7.64%)	15.71 (68.58%)	37.13 (25.74%)	11.36%
		500	500 (0%)	500 (0%)	500 (0%)	380.59 (23.88%)	460.2 (7.96%)	
		5000	5000 (0%)	5000 (0%)	5000 (0%)	4943.58 (1.1%)	4981.2 (0.38%)	
	GSTO + TDE	50	50 (0%)	48.17 (3.66%)	47.78 (4.44%)	11.17 (77.66%)	35.71 (28.59%)	17.35%
		500	500 (0%)	500 (0%)	500 (0%)	232.12 (53.57%)	410.71 (17.86%)	
		5000	5000 (0%)	5000 (0%)	5000 (0%)	4159.54 (16.81%)	4719.85 (5.6%)	
		0%	2.62%	5.86%	63.376%	23.85%		

982 **Table S2.** Population sizes and percentage of population decline across experimentally simulated
 983 conditions.

		Climate Change Scenario			
		Control x2 Initial SD	RCP 8.5 Only Mean	RCP 8.5 Only SD	RCP 8.5 x2 Initial SD
Genetic Correlation	None	499.91 (0.18%)	314.88 (37.04%)	500 (0%)	0.05 (99.99%)
	GSTO	494.24 (1.15 %)	306.26 (38.74%)	500 (0%)	0 (100%)
	TDE	500 (0%)	500 (0%)	500 (0%)	0.93 (99.81%)
	GSTO + TDE	500 (0%)	491.54 (1.69%)	500 (0%)	0.11 (99.97%)

984
 985
 986
 987
 988
 989
 990
 991
 992
 993
 994
 995
 996
 997
 998
 999
 1000
 1001
 1002
 1003
 1004
 1005
 1006

1007 **Table S3.** Changes in the average value of traits conforming a thermal performance curve and in
1008 the average reproductive success across climate change (C.C.), genetic correlations and
1009 generations throughout our simulations. For each pairwise combination generations 0, 5 and 85
1010 are shown to indicate change after the acclimatization period and at the end of environmental
1011 change. Across all simulations, the initial values for CT_{\min} , T_{opt} , CT_{\max} and P_{\max} were the same
1012 and are indicated as “Shared Initial”.
1013

Trait	Climate Change Scenario	Generation	Genetic Correlations (G.C.)				
			None	GSTO	TDE	GSTO + TDE	$\overline{G.C}$
CT_{\min} (°C)	Shared Initial	0	10	10	10	10	10
	RCP 4.5	5	10	11.1	9.97	10.8	10.47
		85	9.49	11.7	9.82	11.4	10.6
	RCP 6	5	10	11	9.98	10.8	10.45
		85	9.58	11.6	9.79	11.3	10.57
	RCP 8.5	5	10	11	10	10.7	10.43
		85	10.3	11.7	9.79	11.5	10.82
	\overline{RCP}	5	10	11.03	9.91	10.76	10.43
		85	9.79	11.67	9.8	11.4	10.66
	T_{opt} (°C)	Shared Initial	0	25	25	25	25
RCP 4.5		5	25.6	25.6	26.4	26	25.9
		85	26.3	26.6	27.9	27	26.95
RCP 6		5	25.7	25.7	26.4	26.1	25.98
		85	26.3	26.6	27.9	27.1	26.98
RCP 8.5		5	25.7	25.6	26.4	26.1	25.95
		85	26.7	26.8	27.8	27.1	27.1
\overline{RCP}		5	25.67	25.63	26.4	26.06	25.43
		85	26.43	26.67	27.86	27.06	26.8
CT_{\max} (°C)		Shared Initial	0	32.5	32.5	32.5	32.5
	RCP 4.5	5	32.8	31.8	32.6	31.8	32.25
		85	33.6	32	32.7	31.1	32.35
	RCP 6	5	32.8	31.8	32.6	31.9	32.28
		85	33.6	32.1	32.8	32.3	32.7
	RCP 8.5	5	32.8	31.8	32.6	31.9	32.28
		85	34.2	32.6	33.2	32.8	33.2
	\overline{RCP}	5	32.8	31.8	32.6	31.86	32.27
		85	33.8	32.23	32.9	32.06	32.75
	P_{\max}	Shared Initial	0	10	10	10	10
RCP 4.5		5	10.3	11.9	11.1	12.3	11.4
		85	10.7	12.5	12.3	13.6	12.28
RCP 6		5	10.4	11.9	11.2	12.3	11.45
		85	10.7	12.6	12.3	13.5	12.28
RCP 8.5		5	10.3	11.9	11.1	12.3	11.4

Reproductive Success		85	10.7	12.4	12.2	13.3	12.15
	$\overline{\text{RCP}}$	5	10.33	11.9	11.16	12.3	11.42
		85	10.7	12.5	12.26	13.46	12.23
	RCP 4.5	0	4.06	4.43	4.86	4.98	4.58
		5	6.82	10.8	9.68	11.9	9.8
		85	4.48	7.07	11.1	10.1	8.19
	RCP 6	0	4.04	4.39	4.81	4.91	4.54
		5	6.88	10.9	9.68	12	9.87
		85	3.4	5.06	10.1	8.37	6.73
	RCP 8.5	0	4.03	4.44	4.85	4.99	4.58
		5	6.53	10.4	9.45	11.6	9.5
		85	0.7	0.45	1.7	1.07	0.98
	$\overline{\text{RCP}}$	0	4.04	4.42	4.84	4.96	4.56
		5	6.74	10.7	9.6	11.83	9.72
		85	2.86	4.19	7.63	6.51	5.29

1014